GEOPHYSICAL RESEARCH LETTERS, VOL. 30, NO. 17, 1898, doi:10.1029/2003GL017578, 2003

The sensitivity of the present-day Atlantic meridional overturning circulation to freshwater forcing

O. H. Otterå,[1,2] H. Drange,[1,2,3] M. Bentsen,[1,2] N. G. Kvamstø,[2,3] and D. Jiang[4]

Received 22 April 2003; accepted 3 July 2003; published 9 September 2003.

[1] Mounting evidence indicates that the Atlantic Meridional Overturning Circulation (AMOC) was strongly reduced during cold climate episodes in the past, possible due to freshwater influx from glacial melting. It is also expected that the freshwater input to high northern latitudes will increase as human-induced global warming continues, with potential impacts on the AMOC. Here we present results from a 150 years sensitivity experiment with the Bergen Climate Model (BCM) for the present-day climate, but with enhanced runoff from the Arctic region throughout the integration. The AMOC drops by 30% over the first 50 years, followed by a gradual recovery. The simulated response indicates that the present-day AMOC might be robust to the isolated effect of enhanced, high-latitude freshwater forcing on a centennial time scale, and that the western tropical North Atlantic may provide key information about the long-term variability, and by that monitoring, of the AMOC. *INDEX TERMS:* 1620 Global Change: Climate dynamics (3309); 4255 Oceanography: General: Numerical modeling; 4267 Oceanography: General: Paleoceanography; 4504 Oceanography: Physical: Air/sea interactions (0312); 3220 Mathematical Geophysics: Nonlinear dynamics. **Citation:** Otterå, O. H., H. Drange, M. Bentsen, N. G. Kvamstø, and D. Jiang, The sensitivity of the present-day Atlantic meridional overturning circulation to freshwater forcing, *Geophys. Res. Lett.*, *30*(17), 1898, doi:10.1029/2003GL017578, 2003.

1. Introduction

[2] A common result from present-day climate simulations performed with climate General Circulation Models (GCMs) is that the freshwater flux into the high latitude oceans will increase in response to enhanced greenhouse gas forcing [*Räisänen*, 2001]. It is still unclear, however, how sensitive the present-day climate GCMs are to a strong increase in the freshwater flux.

[3] To examine the transient response to anomalous freshwater input to the northern high latitude oceans for the present-day climate, a twin experiment with the newly developed BCM (see Sec. 2) has been conducted. The basis for the experiment is a 300 yr control (CTRL) integration with greenhouse gas and aerosol particle concentrations kept at the present-day values [*Furevik et al.*, 2003]. The simulated continental freshwater flux to the Nordic Seas and the Arctic Ocean in CTRL is 0.1 Sv (1 Sv = 10^6 m^3 s^{-1}), a value consistent with observational based estimates [*Aagaard and Carmack*, 1989]. The freshwater (FW) experiment, starting from year 100 of CTRL, is governed by an artificially threefold increase in the freshwater flux to the Nordic Seas and the Arctic Ocean throughout the simulation. For comparison, FW represents a perturbation of the system similar to the simulated increase in the freshwater input poleward of 50° N obtained at a quadrupling of the pre-industrial CO_2 level [*Manabe and Stouffer*, 1997]. The freshwater flux is also believed to be consistent with the meltwater entering the high northern oceans during the last deglaciation [*Simonsen*, 1996]. Both comparisons illustrate that the applied freshwater flux is strong. In addition, the increased freshwater flux has been artificially added to the system in contrast to a full climate-change scenario with an internally consistent hydrological cycle, so the performed integration should be viewed as a sensitivity experiment only.

2. Model Description

[4] BCM [*Furevik et al.*, 2003] consists of the atmosphere General Circulation Model (GCM) ARPEGE/IFS [*Déqué et al.*, 1994] and the ocean GCM MICOM [*Bleck et al.*, 1992], the latter coupled with a dynamic and thermodynamic sea ice model. ARPEGE/IFS is run in a linear T_L63 grid (horizontal resolution is about 2.8-by-2.8 degrees) with 31 vertical levels, ranging from the surface to 0.01 hPa. The version used in BCM differs from the version in *Déqué et al.* [1994] by the following features [*Furevik et al.*, 2003]: It contains a convective gravity drag parameterisation, a new snow scheme, increased orographic drag and modifications in deep convection and soil vegetation schemes.

[5] MICOM is run with a horizontal Mercator grid mesh with one pole over Siberia and the other over Antarctica, and with a nominal resolution of 2.4-by-2.4 degrees. The horizontal resolution is increased to 0.8 degrees in a band along the Equator to better resolve equatorial-confined dynamics. The model has 24 layers in the vertical, with an uppermost mixed layer with temporal and spatial varying density, and 23 isopycnal layers below with potential densities ranging from 24.12 to 28.10.

[6] To avoid drift from climatological sea surface temperature and salinity fields, the heat and fresh water fluxes are adjusted based on a time-invariant flux-correction derived from the spin-up of the model [*Furevik et al.*, 2003]. The increased freshwater flux in FW has been incorporated by multiplying the fresh water runoff to the Nordic Seas and the Arctic Ocean by a factor four.

[1]Nansen Environmental and Remote Sensing Center, Bergen, Norway.
[2]Bjerknes Centre for Climate Research, Bergen, Norway.
[3]Geophysical Institute, University of Bergen, Bergen, Norway.
[4]LASG, Institute of Atmospheric Physics, Chinese Acadamy of Sciences, Beijing, China.

0094-8276/03/2003GL017578$05.00

3. Results and Discussion

[7] The maximum AMOC in CTRL shows decadal variations of 1.5 Sv, and a mean value of about 18 Sv (Figure 1a), which is close to the mean value of 15 other climate GCMs [*Lambert and Boer*, 2001]. The northward heat transport (relative to 0°C) at 24°N in CTRL is 0.95 PW, a value that is on the low end of observational-based estimates [*Hall and Bryden*, 1982]. Furthermore, the simulated poleward transport of Atlantic Water (AW) across the Greenland-Scotland Ridge (GSR) is 8.2 Sv (8.0 Sv based on observations from *Hansen and Østerhus* [2000]), and the northeastward transport of Atlantic and coastal waters into the Barents Sea is 2.6 Sv (2.5 Sv; *Schauer et al.* [2002] and *Ingvaldsen et al.* [2002]). In addition, the poleward flow of Pacific Water through the Bering Strait is 1.3 Sv, and the southward flow through the Canadian Archipelago is 1.6 Sv. These diagnostics yield credibility to CTRL and the model system for the present-day climate.

[8] The response to the added freshwater can be split into a freshening phase (Phase 1, hereafter P1, covering year 1–50) and a recovery phase (P2, subsequent 100 years). The direct responses in P1 are 1) reduced sea surface salinity and temperature over most of the North Atlantic (NA), 2) suppressed variability and reduced winter-time deepwater formation rates in the NA sub-polar gyre (here defined as the Labrador and Irminger Seas) and in the Nordic Seas (Figure 1b), 3) increased extent of sea ice in the Labrador and Barents Seas, 4) a cooling of more than 1.5°C poleward of 30°N (Figure 2a), and 5) a tendency for an increased sea level pressure (SLP) difference between Iceland and Spain (Figure 2c).

[9] The poleward flow of AW between Greenland and the Faroes is reduced by 1.5 Sv in P1, whereas the poleward flow through the Faroe-Shetland Channel is close to CTRL. The latter response is attributed to the SLP anomaly (Figure 2c) in FW [*Nilsen et al.*, 2003]. Furthermore, the flow of water into the Barents Sea drops by 1 Sv. Observations show that the AW entering the Arctic Ocean from the shallow Barents Sea is cold, saline and dense, and therefore intrudes the Arctic Ocean at intermediate depths [*Schauer et al.*, 2002; *Mauritzen*, 1996]. This is also the case in CTRL, whereas the reduced flow of waters from the Barents Sea to the Arctic Ocean in FW is the main reason for the reduced southward sub-surface flow of 1.5 Sv through the Fram Strait (Figure 1b). The change in the sub-surface flow through the Fram Strait, together with weaker winter-mixing in the Nordic Seas (Figure 1b), lead to a reduced overflow of 1.7 Sv across GSR (Figure 1b). The reduced overflow, combined with less intense winter-mixing in the NA sub-polar gyre (Figure 1b), are the main causes for the ~6 Sv drop in AMOC in P1 (Figure 1a).

[10] With reduced formation of dense water masses in the northern NA, the vertical density stratification in the Atlantic Ocean weaken with time. Theory and open ocean studies [*Gargett*, 1984] indicate that the strength of the diapycnal mixing can be parameterised as proportional to $N^{-\alpha}$, where

$$N = (g/\rho|\partial\rho/dz|)^{1/2}$$

is the Brunt-Väisälä frequency (s^{-1}) and α is a parameter close to unity (here g (m s^{-2}) is gravity, ρ (kg m^{-3}) is density, and z (m) is depth). In BCM, the diapycnal mixing coefficient is given by $3 \times 10^{-7} N^{-1}$ (m^2 s^{-1}), hence the diapycnal mixing increases with decreasing vertical density stratification.

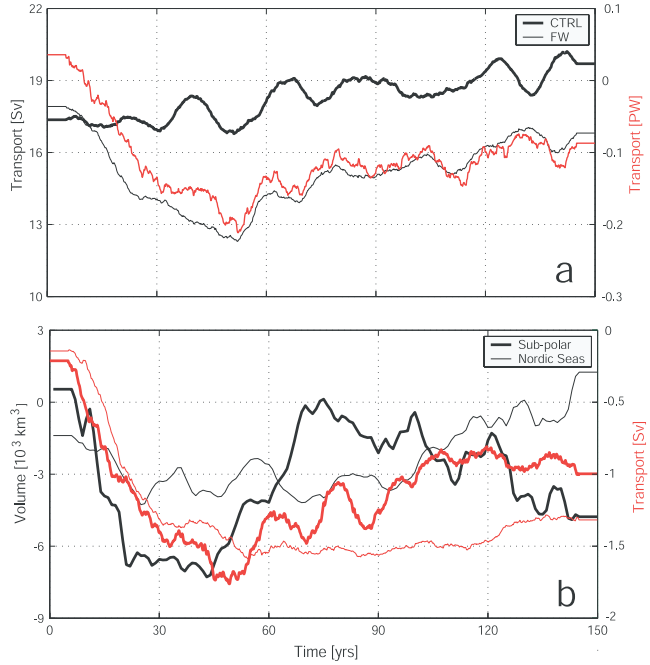

Figure 1. Basic characteristics of the AMOC. Time series of 10-year running means of (a) the maximum AMOC (Sv, black curves) in CTRL and FW, and the anomaly in the northward heat transport (PW, red curve) at 24°N, and (b) the anomaly in the mean volume (km^3, black curves) of the mixed layer waters that mixes below 500 m in March in the NA sub-polar gyre and in the Nordic Seas, and the anomalies in the southward transport (Sv) of waters with potential density >27.4 through the Fram Strait (thin red curve) and across GSR (thick red curve). The mixing regions in (b) are defined as the regions where the surface mixing in March exceeds 1500 m at least once during either CTRL or FW. The anomalies are based on the difference FW-⟨CTRL⟩, where ⟨CTRL⟩ is the second-order polynomial least-square fit to the 150 years CTRL integration.

[11] The zonally averaged change in the strength of the diapycnal mixing is provided in Figure 3. In the first half of P2, here taken as the period between years 71–90, the diapycnal mixing in FW increases by 5–10% over a substantial part of the Atlantic Basin. From scaling arguments and numerical simulations [*Nilsson and Walin*, 2001; *Nilsson et al.*, 2003], the diapycnal upwelling is proportional to N^{-1} for a diapycnal mixing coefficient proportional to N^{-1}. The AMOC is estimated to increase by about 1 Sv, or 25%, as a result of the 5–10% increased diapycnal mixing, and by that basin-scale diapycnal upwelling [*Nilsson and Walin*, 2001], in FW.

[12] Phase 2 is further governed by a gradual increase in salinity and temperature of the surface and sub-surface waters at low latitudes. For essentially unchanged surface air temperatures, as is the case in FW south of 20°N (Figure 2a), the residence time of the surface water determines the accumulated effect of the heat and fresh water fluxes. At the end of P1 in FW, the annual mean speed of

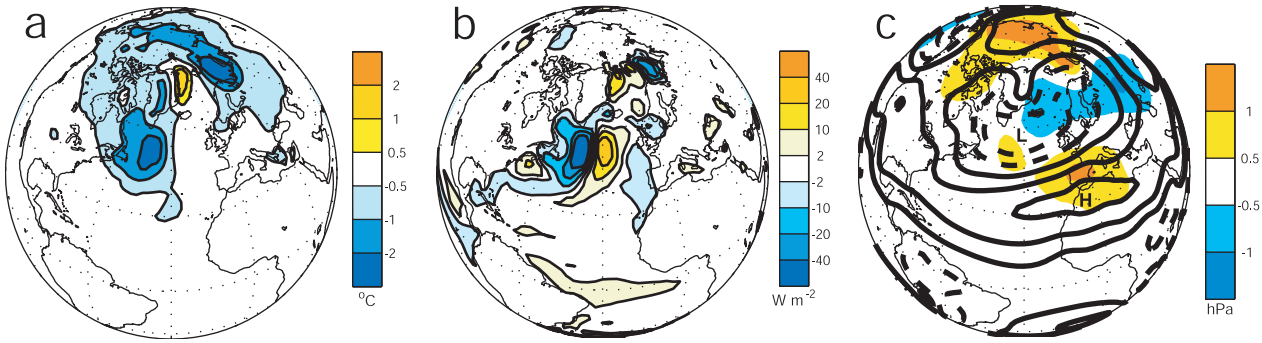

Figure 2. Simulated atmospheric responses. (a) and (b) give the anomalies in annual mean surface air temperature (°C) and annual mean net heat flux (W m^{-2}) for year 31–90, respectively. The winter (Dec–Feb) SLP anomaly is fairly stable throughout the integration. Therefore, (c) shows the winter SLP (hPa; lines) and SLP anomaly (hPa; coloured) averaged over the entire integration. All anomalies are computed as the difference FW-CTRL. Positive values in (b) mean net flux of heat from the ocean. Contour interval for the isobars in (c) are 5 hPa, with 1005 and 1010 hPa dashed. For comparison, one standard deviation (std) in the annual mean surface air temperature in CTRL is <0.5°C over ocean and about 1°C over land poleward of 50°N. For the annual mean net heat flux, the variability in CTRL is largest over the ocean with one std of about 10 W m^{-2} in the western part of the North Atlantic Ocean/Nordic Seas.

the uppermost 600 m of the Guyana Current is reduced by 0.014 m s^{-1} (Figure 4a), or by 25% compared to the mean value of 0.057 m s^{-1} in CTRL. The reduced flow speed in FW corresponds to an increased travel time of 8 months along the 4.7×10^6 m long northeastern coast of South America. This leads to positive salinity and temperature anomalies of up to 0.2 psu and 0.8°C averaged over the uppermost 600 m of the water column in the western tropical NA (Figures 4a–4c). Increased salinity and temperature are also obtained in the South Atlantic sub-tropical gyre (Figure 4b).

[13] Gradually, the anomalously warm and saline waters are carried northward with the North Atlantic Drift (NAD) following a more eastward path than in CTRL (Figure 2b). During the first half of P2, the salt transported by the NAD makes the surface water sufficiently dense to support winter-mixing both in the NA sub-polar gyre and in the Nordic Seas (Figure 1b). The net inflow to the Nordic Seas increases throughout P2, and is only 0.3 Sv, on average, below CTRL over the last 50 years. The recovery is further characterised by: 1) About 0.5 Sv increase in the transport of AW through the Faroe-Shetland Channel and into the Barents Sea, 2) a weak increase in the southward sub-surface flow through the Fram Strait (Figure 1b), 3) an increased poleward transport of AW through the Fram Strait of about 0.4 Sv, 4) a warming in the Fram Strait region (Figures 2a and 2b), and 5) a winter-mixing in the Nordic Seas comparable to or slightly exceeding that of CTRL (Figure 1b). The net effect of 2) and 5) is an increase in the overflow across GSR in P2 of about 0.8 Sv (Figure 1b). The mass budget for the Nordic Seas-Arctic Ocean is closed with a reduced inflow of 0.3 Sv through the Bering Strait and a similar increase in the southward flow through the Canadian Archipelago.

[14] During P2, the surface air temperature anomaly poleward of 45°N reduces from −0.3°C to −0.1°C in response to the general increase in the ocean transport of heat (Figure 1a), possibly in combination with an atmosphere Rossby wave response.

[15] In parallel with the strengthened AMOC, the Guyana Current intensifies, and the formation of warm and saline waters in the South Atlantic and in the western tropical NA gradually diminishes (Figure 4c). As a result, the ocean transport of salt by the eastward-shifted NAD is not sufficient to counteract the continuous supply of freshwater. This leads to reduced mixing in the NA sub-polar region in the second half of P2 (Figure 1b), contributing to an ocean state tending to run into a new freshening phase. However, the trend in the overflow across GSR remains positive to year 120 (Figure 1b), and the overall supply of abyssal waters in P2 leads to a vertical density stratification, and by that a basin-scale diapycnal upwelling, close to CTRL.

4. Concluding Remarks

[16] The performed twin-experiment illustrates some non-linear and perhaps non-intuitive interactions in the climate system in the Atlantic-Arctic region, including the importance of the local winds on the flow of AW into the Nordic Seas [*Nilsen et al.*, 2003], the role of the Barents Sea and the deep flow through the Fram Strait as mediators

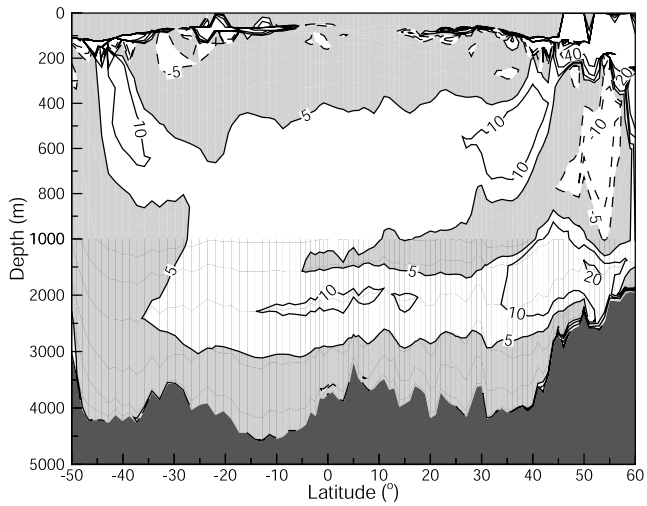

Figure 3. The difference in % of the zonal mean value of the diapycnal mixing in the Atlantic Ocean for year 71–90.

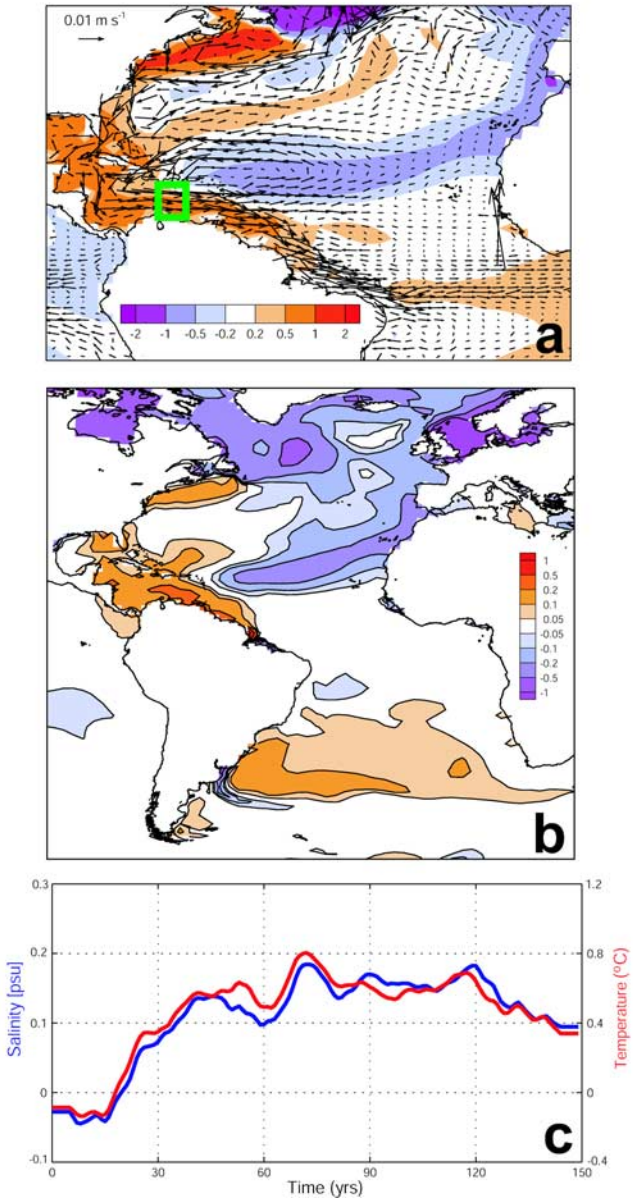

Figure 4. Simulated ocean responses. The anomalies (FW-CTRL) in (a) annual mean temperature (°C) and velocity and (b) annual mean salinity (psu) for year 50. (c) Shows the anomalies (FW-⟨CTRL⟩) in temperature (°C, red curve) and salinity (psu, blue curve) averaged over the box in (a), and computed as in Figure 1. All of the anomalies are averaged over the upper 600 m of the water column. Reference vector for the velocity field is provided in the upper left corner of (a).

of the GSR overflow [*Mauritzen*, 1996], the hitherto untested response of density stratification dependent diapycnal mixing [*Gargett*, 1984; *Nilsson and Walin*, 2001; *Nilsson et al.*, 2003] on AMOC in climate GCMs, and the coupling between tropical heat and salt anomalies and high-latitude winter-mixing [*Manabe and Stouffer*, 1997]. The tropical anomalies in FW are consistent with key observations of oceanic responses during the rapid climate changes of the last deglaciation: That anomalously high surface temperatures in the western tropical NA coincides with intense cooling—and presumably with weakened AMOC—at higher latitudes [*Rühlemann et al.*, 1999]. The model experiment propose an approximately century-scale variability mode in the Atlantic which is linked to the formation and decay of the western tropical anomalies (Figures 4a–4c), highlighting the importance of this region for detecting large-scale changes of the past [*Rühlemann et al.*, 1999], and the possibility for monitoring of the modern AMOC.

[17] **Acknowledgments.** The study has been supported by the Research Council of Norway through a personal grant to O.H.O., through RegClim (H.D.), KlimaProg's "Spissforskningsmidler" (M.B.) and the Program of Supercomputing, by the National Natural Science Foundation of China under grant 40125014 (D.J.), by the EU-project PREDICATE (EVK2-CT-1999-00020), and by the G. C. Rieber Foundations. The authors are grateful to the BCM group for help and guidance. This is contribution no. A0026 from the Bjerknes Centre for Climate Research.

References

Aagaard, K., and E. C. Carmack, The role of sea ice and other fresh water in the Arctic Circulation, *J. Geophys. Res.*, *94*, 14,485–14,498, 1989.

Alley, R. B., Paleoclimatology: Icing the North Atlantic, *Nature*, *392*, 335–337, 1998.

Bleck, R., C. Rooth, D. Hu, and L. T. Smith, Salinity-driven Thermocline Transients in a Wind- and Thermohaline-forced Isopycnic Coordinate Model of the North Atlantic, *J. Phys. Oceanogr.*, *22*, 1486–1505, 1992.

Déqué, M., C. Dreveton, A. Braun, and D. Cariolle, The ARPEGE/IFS atmosphere model: A contribution to the French community climate modelling, *Clim. Dyn.*, *10*, 249–266, 1994.

Furevik, T., M. Bentsen, H. Drange, I. K. T. Kindem, N. G. Kvamstø, and A. Sorteberg, Description and validation of the Bergen Climate Model: ARPEGE coupled with MICOM, *Clim. Dyn.*, *21*, 27–51, doi:10.1007/300382-003-0317-5, 2003.

Gargett, A. E., Vertical eddy diffusivity in the ocean interior, *J. Marine Res.*, *42*, 359–393, 1984.

Hall, M. M., and H. L. Bryden, Direct estimates and mechanisms of ocean heat transport, *Deep Sea Res.*, *29*, 339–359, 1982.

Hansen, B., and S. Østerhus, North Atlantic - Nordic Seas exchanges, *Prog. Oceanogr.*, *45*, 109–208, 2000.

Ingvaldsen, R., H. Loeng, and L. Asplin, Variability in the Atlantic inflow to the Barents Sea based on a one-year time series from moored current meters, *Cont. Shelf Res.*, *22*, 505–519, 2002.

Lambert, S. J., and G. J. Boer, CMIP1 evaluation and intercomparison of coupled climate models, *Clim. Dyn.*, *17*, 83–106, 2001.

Manabe, S., and R. J. Stouffer, Coupled ocean-atmosphere model response to freshwater input: Comparison to Younger Dryas event, *Paleoceanography*, *12*, 321–336, 1997.

Mauritzen, C., Production of dense overflow waters feeding the North Atlantic across the Greenland-Scotland Ridge. Part 1: Evidence for a revised circulation scheme, *Deep Sea Res.*, *43*, 769–806, 1996.

Nilsen, J. E. Ø., Y. Gao, H. Drange, T. Furevik, and M. Bentsen, Simulated North Atlantic-Nordic Seas water mass exchanges in an isopycnic coordinate OGCM, *Geophys. Res. Lett.*, *30*, doi:10.1029/2002GL016597, 2003.

Nilsson, J., and G. Walin, Freshwater forcing as a booster of thermohaline circulation, *Tellus*, *53*(5), 629–641, 2001.

Nilsson, J., G. Broström, and G. Walin, The thermohaline circulation and vertical mixing: Does weaker density stratification give stronger overturning?, *J. Phys. Oceanogr*, in press, 2003.

Räisänen, J., CO_2-induced climate change in the Arctic area in the CMIP2 experiments, *SWECLIM Newsletter*, *11*, 23–28, 2001.

Rühlemann, C., S. Mulitza, P. J. Müller, G. Wefer, and R. Zahn, Warming of the tropical Atlantic Ocean and slowdown of thermohaline circulation during the last deglaciation, *Nature*, *402*, 511–514, 1999.

Schauer, U., H. Loeng, B. Rudels, V. K. Ozhigin, and W. Dieck, Atlantic Water flow through the Barents and Kara Seas, *Deep Sea Res.*, *49*, 2281–2298, 2002.

Simonsen, K., Heatbudgets and freshwater forcing of the Nordic Seas and the Arctic Ocean, Ph.D. thesis, Nansen Env. and Remote Sensing Center, Bergen, Norway, 1996.

O. H. Otterå, H. Drange, and M. Bentsen, Nansen Environmental and Remote Sensing Center, Edvard Griegsvei 3A, 5059 Bergen, Norway. (oddho@nersc.no)

N. G. Kvamstø, Geophysical Institute, University of Bergen, Allègt. 70, 5007 Bergen, Norway.

D. Jiang, LASG, Institute of Atmospheric Physics, Chinese Acadamy of Sciences, Beijing 100029, China.